

Complete temporal characterization of a single photon

Zhongzhong Qin,^{1,2} Adarsh S. Prasad,¹ Travis Brannan,¹ Andrew MacRae,³ A. Lezama,⁴ and A. I. Lvovsky^{1,5,*}

¹*Institute for Quantum Science and Technology,
University of Calgary, Alberta T2N1N4, Canada*

²*Quantum Institute for Light and Atoms, State Key Laboratory of Precision Spectroscopy,
East China Normal University, Shanghai 200062, People's Republic of China*

³*Department of Physics, University of California, Berkeley, California 94720, USA*

⁴*Instituto de Física, Facultad de Ingeniería, Universidad de la República,
J. Herrera y Reissig 565, Montevideo 11300, Uruguay*

⁵*Russian Quantum Centre, 100 Novaya St., Skolkovo, Moscow 143025, Moscow, Russia*
(Dated: December 3, 2024)

Abstract

Precise information about the temporal mode of optical states is crucial for optimizing their interaction efficiency between themselves and/or with matter in various quantum communication devices. Here we propose and experimentally demonstrate a method of determining both the real and imaginary components of a single photon's temporal density matrix by measuring the autocorrelation function of the photocurrent from a balanced homodyne detector at multiple local oscillator frequencies. We test our method on single photons heralded from biphotons generated via four-wave mixing in an atomic vapor and obtain excellent agreement with theoretical predictions for several settings.

Single photons and single photon qubits are among the foundations of most quantum optical information processing techniques such as cryptography [1], teleportation [2], repeaters [3] and computing [4]. Many of these applications require the photons to have a well-defined, pure modal structure. Possessing precise information about that structure is essential for quantum-optical technology.

An approximate guess of a photon's mode can be inferred theoretically from the characteristics of the source [5–9], but this information is not always available or reliable. For example, this approach would not work for photons sent in by a remote party in a communication scheme, or for photons from an incompletely characterized mesoscopic source. Therefore, it is important to have a technique for precise characterization of a photon's mode experimentally. While such techniques are relatively well developed for spatial modes [10, 11], their extension into the temporal domain is challenging.

Complete information about a photon's temporal properties can be obtained by studying its interference with a classical field. Polycarpou *et al.* used adaptive waveform shaping of local oscillator (LO) pulses [12] to heuristically find the LO temporal mode that maximizes the efficiency of homodyne detection of the photon. This occurs when the LO temporal mode matches that of the signal, enabling measurement of that mode. However, physical shaping of LO pulses is quite sophisticated experimentally. Furthermore, this technique has only been demonstrated for pure temporal modes.

If the photon mode is not ultrashort (i.e. it can be resolved by the detection electronics), the physical matching of the LO to the signal can be replaced by analyzing the time-resolved statistics of the homodyne detector's output photocurrent with a continuous-wave LO.

MacRae *et al.* [13, 17] showed that the autocorrelation function of this photocurrent estimates the real part of the density matrix defining the photon's temporal mode. Subsequently, this approach has been utilized for the “Schrödinger cat” and two-photon Fock states [15].

However, the method proposed by MacRae *et al.* does not yield any information about the imaginary part of the photon's temporal density matrix (TDM), and hence, does not completely characterize the mode. In this paper we present an experimental technique of *polychromatic optical heterodyne tomography*, which relies on acquiring the autocorrelation data of the homodyne photocurrent at multiple LO frequencies. The method enables us to determine both the real and imaginary parts of the photon's TDM, thereby completely characterizing its temporal state. It works equally well for pure and mixed temporal modes.

The (pure) temporal mode of a photon is defined by annihilation operator

$$\hat{A}_\phi = \int_{-\infty}^{\infty} \hat{a}_t \phi(t) dt, \quad (1)$$

where $\phi(t)$ is the temporal mode function (TMF) and \hat{a}_t represents the instantaneous annihilation operator at time t [16]. A single photon state in this mode is then given by $|1_\phi\rangle = \hat{A}_\phi^\dagger |0\rangle = \int_{-\infty}^{\infty} \phi^*(t) |1_t\rangle dt$, where $|1_t\rangle = \hat{a}_t^\dagger |0\rangle$.

The digital nature of the data acquisition system used in our experiment compels us to represent the temporal modes in terms of discrete time bins. The single photon state in temporal mode $\phi(t)$ can then be approximately expressed as $|1_\phi\rangle = \sum_j \phi^*(t_j) |1_j\rangle$ with $\sum_j |\phi(t_j)|^2 = 1$. Here t_j is the time associated with the j^{th} bin and $|1_j\rangle$ is the state containing one photon in the top-hat temporal mode associated with the j^{th} bin and vacuum

in all other bins. The density operator of the photon is then represented as $\sum_{mn} \rho_{mn} |1_m\rangle \langle 1_n|$ where ρ_{mn} is the temporal density matrix.

The homodyne current for the j^{th} time bin $I(t_j)$ is proportional to the quadrature

$$\hat{X}_j = (\hat{a}_j e^{-i\theta_j} + \hat{a}_j^\dagger e^{i\theta_j})/\sqrt{2}, \quad (2)$$

where $\theta_j = \delta\omega \cdot t_j + \theta_0$ is the optical phase difference between the LO and the signal. Here $\delta\omega$ is the frequency detuning between the LO and the signal and θ_0 the LO relative phase at $t = 0$. The autocorrelation matrix for the homodyne current is then

$$\begin{aligned} \langle I(t_j) I(t_k) \rangle &\propto \langle \hat{X}_j \hat{X}_k \rangle = \text{Tr}[\hat{\rho} \hat{X}_j \hat{X}_k] \\ &= \sum_{mn} \rho_{mn} \langle 1_n | \hat{X}_j \hat{X}_k | 1_m \rangle, \end{aligned} \quad (3)$$

where each matrix element can be evaluated using Eq. (2) as

$$\begin{aligned} \langle 1_n | \hat{X}_j \hat{X}_k | 1_m \rangle & \\ = \frac{1}{2} \left[e^{-i\delta\omega(t_k - t_j)} \delta_{km} \delta_{nj} + \delta_{jk} \delta_{nm} + e^{-i\delta\omega(t_j - t_k)} \delta_{jm} \delta_{nk} \right]. \end{aligned} \quad (4)$$

Note that Eq. (4) does not depend on θ_0 due to the phase uncertainty of Fock states.

From Eqs. (3) and (4), one can obtain

$$\langle \hat{X}_j \hat{X}_k \rangle = \frac{1}{2} \delta_{jk} + A_{jk}. \quad (5)$$

The first term in Eq. (5) corresponds to the autocorrelation matrix for the vacuum. The second term, which we call the *reduced* autocorrelation matrix, is directly related to the photon's TDM:

$$A_{jk} = \text{Re}[\rho_{jk}] \cos[\delta\omega(t_j - t_k)] + \text{Im}[\rho_{jk}] \sin[\delta\omega(t_j - t_k)]. \quad (6)$$

If the LO frequency is same as that of the signal, i.e., at $\delta\omega = 0$, the autocorrelation matrix depends only on the real part of the TDM. However, by using $\delta\omega \neq 0$ one obtains access to its imaginary part.

Our experimental scheme for creating the single-photon state and measuring the autocorrelation matrix is shown in Fig. 1. We use coherent double Raman scattering (four-wave mixing) in an ensemble of Λ -type atoms to generate a two-mode squeezed state in a non-degenerate phase-matched configuration [17]. A hot ^{85}Rb vapor cell is pumped by a 1 Watt laser beam at 795 nm derived from a continuous-wave Ti:Sapphire laser. The signal and idler beams are spatially separated from the pump, and a specific spatial mode is selected in the idler channel using a single-mode fiber. Subsequently, the idler channel is subjected to spectral filtering by means of a lens cavity (C1) of a 55 MHz bandwidth [18] and a conventional Fabri-Perot cavity (C2) of bandwidth $\gamma/2\pi = 7$

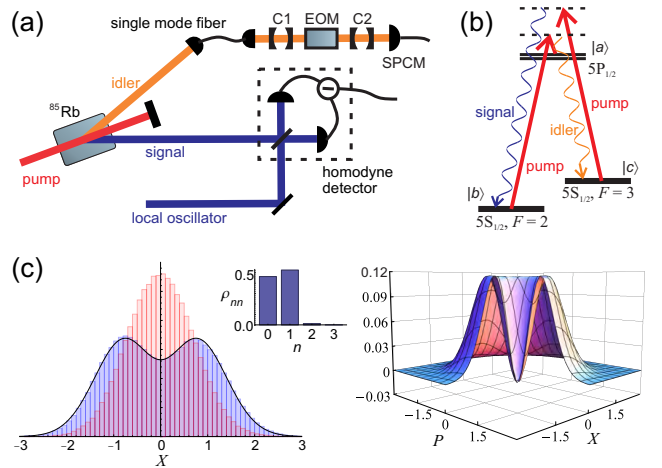


FIG. 1. (a) Schematic of the experimental set-up (C1, C2: filter cavities; EOM: electro-optic modulator; SPCM: single photon counting module). The signal (blue) goes to the homodyne detector, whereas the idler (orange) passes through C1 (55 MHz) and C2 (7 MHz) before detection via the SPCM. The EOM between C1 and C2 is optional. (b) The ^{85}Rb three-level Λ system, with the fields' configuration shown. (c) Reconstruction of the state of the electromagnetic field in the temporal mode determined experimentally (unmodulated case). Left to right: experimental quadrature distribution (blue) overlaid with that for the vacuum state (red); diagonal elements of the Fock-basis density matrix; Wigner function. The single-photon fraction is 52.6%.

MHz. The usage of two cavities with incommensurate free spectral ranges ensures that the combined spectral filter has a single transmission peak of 7 MHz width.

The idler beam is then coupled to a PerkinElmer single photon counting module (SPCM) with a dark count rate below 100 Hz. Both cavities are maintained at a stable frequency by using an alignment beam which is unblocked every few seconds to monitor and readjust the cavity resonance frequency. Detection of an idler photon projects the signal onto a single photon in a well-defined spatio-temporal mode conjugate to the idler. This signal channel is mode-matched with a continuous-wave LO (18 mW) for homodyne detection [19]. The LO is derived from a diode laser that is locked and phase stabilized with respect to the pump using an optical phase-lock loop [20].

A click from the SPCM in the idler channel acts as the trigger for the measurement of the signal. The homodyne photocurrent is recorded for 360 ns around the trigger point as reference with a time binning of 2 ns. For each LO detuning, the autocorrelation matrix (3) of the homodyne photocurrent is obtained by taking an average over 2 million traces.

Theoretically, the data corresponding to two LO detunings would constitute a quorum for the temporal mode reconstruction. Experimentally, however, we take data at eight different detunings to avoid the situation

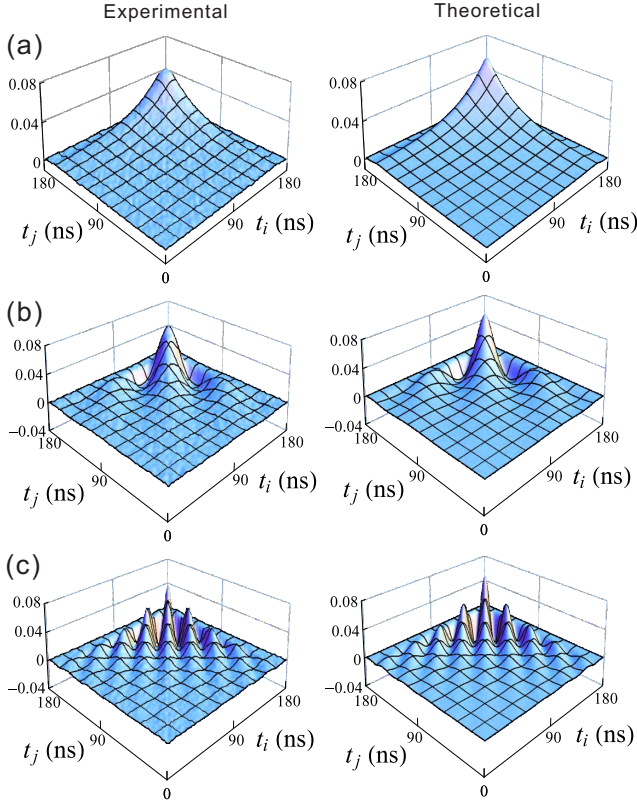


FIG. 2. Theoretical (right) and experimental (left) reduced autocorrelation matrices, for three different LO detunings: (a) 0 MHz, (b) -10.8 MHz, and (c) 27 MHz, corresponding to the measurement setting without modulation. The trigger photon arrives at $t = 155$ ns.

where the sinusoids in Eq. (6) approach zero for all detunings simultaneously. This allows for recovery of $\hat{\rho}$ with minimum uncertainty.

Once the autocorrelation matrices have been acquired, we process them to eliminate the vacuum term in Eq. (5), as well as any contributions from the DC bias in the homodyne photocurrent and thermal background. These contributions are not correlated with trigger events, and are only dependent on the difference $t_j - t_k$. They can therefore be evaluated as the mean autocorrelation value along lines $t_j - t_k = \text{const}$ for the data points acquired significantly after the trigger pulse where no signal photon is expected. Subtracting them from the autocorrelation matrix yields the reduced autocorrelation matrix (Fig. 2).

The TDM can now be determined by solving Eq. (6) for each pair (j, k) . However, such direct approach does not ensure positivity and normalization of the reconstructed density operator. To incorporate these *a priori* constraints into the reconstruction, we implement a more sophisticated iterative optimization algorithm. The algorithm uses the eight experimental reduced autocorrelation matrices as the training set. The difference be-

tween the experimental left-hand side of Eq. (6) and the right-hand side of that equation evaluated from the estimated TDM, squared and summed over all pairs (j, k) and all LO frequencies, is used as the cost function. Iterations utilize the diagonal representation of the TDM: $\hat{\rho} = \sum_i p_i |\psi_i\rangle \langle \psi_i|$. In the first step of each iteration, the eigenvalues p_i are adjusted to minimize the cost function while keeping them real, non-negative and totalling 1. In the second step, the eigenvectors $|\psi_i\rangle$ are optimized by pairwise unitary transformations. The process is repeated until the cost function asymptotically converges to give the best fit of the TDM.

The theoretically expected mode is calculated from the properties of our experimental setup. The primary element determining the mode of the heralded photon is the narrowband filter cavity C2 in the idler channel. Additionally, the mode's bandwidth is limited by the ~ 50 MHz gain bandwidth of the four-wave mixing process used to generate the biphotons. This effect is taken into account in theoretical plots in Figs. 2 and 3, however we neglect it in the theoretical expressions below for clarity.

The Lorentzian filter C2 in the idler channel produces a signal photon with the TMF in the shape of a rising exponential that terminates at the trigger event [21]:

$$\phi(t) = \sqrt{\gamma} e^{\gamma t/2} \Theta(-t), \quad (7)$$

where $\Theta(t)$ is the Heaviside step function and $\gamma = 2\pi \times 7$ MHz is the narrowband cavity linewidth.

Fig. 3(a) shows the TDM obtained by iterative reconstruction from the experimental data along with the theoretical predictions. The primary eigenvector of the TDM has a corresponding eigenvalue almost 45 times larger than the second largest one indicating a nearly pure temporal mode. The TDM is primarily real and matches well the theoretical prediction. The observed artifacts can be attributed to the effect of applying the reconstruction algorithm to imperfect experimental data that are affected by noise and finite response times.

Next, we demonstrate the reconstruction of a temporal mode with a nonvanishing imaginary component. To this end, we induce a virtual phase modulation by redefining the signal-LO detuning according to $\delta\omega' = \delta\omega + \Delta$ when reconstructing the TDM from Eq. (6). The theoretically expected TMF and TDM then become:

$$\phi^{\text{shifted}}(t) = \phi(t) e^{i\Delta t}; \quad (8)$$

$$\rho^{\text{shifted}}(t, t') = \rho(t, t') e^{i\Delta(t-t')}. \quad (9)$$

The TDM reconstructed from the experimental data using the effective modulation frequency of $\Delta = 2\pi \times 5$ MHz is shown in Fig. 3(b). While the purity of the temporal mode is maintained, the reconstructed density matrix now has a significant imaginary component, demonstrating the ability of our technique to accurately reconstruct states with complex temporal modes.

Finally, we illustrate the ability of the experimental technique to reconstruct the TDM in the case of a mixed state. We phase modulate the signal photons at a frequency $\omega_m = 2\pi \times 20$ MHz, larger than the spectral width of C2. This is achieved by passing the idler photons through an electro-optic modulator (EOM), with its optical axis oriented along the photon's polarization [22]. This leads to a TMF $\phi^{\text{EOM}}(t, \theta_m) = \sqrt{\gamma} e^{\gamma t/2} e^{i\beta \sin(w_m t + \theta_m)} \Theta(-t)$, where $\beta = 1.1$ is the modulation index and θ_m is the phase of the modulating voltage at the time when the idler photon is detected. Because the idler photon detections occur at random times, θ_m is randomized, leading to the following non-pure TDM:

$$\begin{aligned} \rho_{t,t'}^{\text{EOM}} &= \frac{1}{2\pi} \int_{-\pi}^{\pi} [\phi^{\text{EOM}}(t, \theta_m)]^* \phi^{\text{EOM}}(t', \theta_m) d\theta_m \quad (10) \\ &= \gamma e^{\frac{\gamma(t+t')}{2}} \Theta(-t) \Theta(-t') J_0 \left[2\beta \sin \left(\frac{\omega_m(t-t')}{2} \right) \right], \end{aligned}$$

where J_0 is the Bessel function of the first kind.

The experimentally reconstructed TDM is shown in Fig. 3(c). The mixed nature of the density matrix is evident from the distribution of eigenvalues, with the ratio of the first and second eigenvalues being only around 2. Due to the modulation phase randomization, the imaginary part of the density matrix is zero.

The fidelity of the experimentally obtained TDMs, defined as $F = \text{Tr}[\sqrt{\sqrt{\rho_{\text{exp}}} \rho_{\text{th}} \sqrt{\rho_{\text{exp}}}}]$ with subscripts indicating theory versus experiment, is calculated for the three cases (without modulation, with virtual modulation, and with EOM modulation) to be 0.97, 0.94 and 0.93 respectively. Using the TMF obtained for the unmodulated case [Fig. 3(a)], we reconstruct the quantum state of light in that mode in the Fock basis akin to Ref. [17], obtaining the single-photon efficiency of $\rho_{11} = 52.6\%$, showing improvement over our previous results [17]. The corresponding Wigner function, exhibiting negative values at the phase-space origin, is plotted in Fig. 1(c) along with the acquired quadrature distribution and the reconstructed density matrix.

In summary, we have developed and experimentally demonstrated polychromatic optical heterodyne tomography, a robust method for complete experimental determination of the temporal properties of a single photon directly from the time-resolved photocurrent statistics of a balanced homodyne measurement. The method enables the extraction of a temporal mode which in general may be complex and can have multiple frequency components. Accurate detection of the temporal mode is key for the proper mode matching required by many quantum communication protocols, and enables high efficiency tomographic reconstruction of the quantum optical state in the channel of interest.

ZQ and ASP contributed equally to this work. The authors thank Erhan Saglamyurek and Wolfgang Tittel for lending us the EOM. The project is supported by NSERC

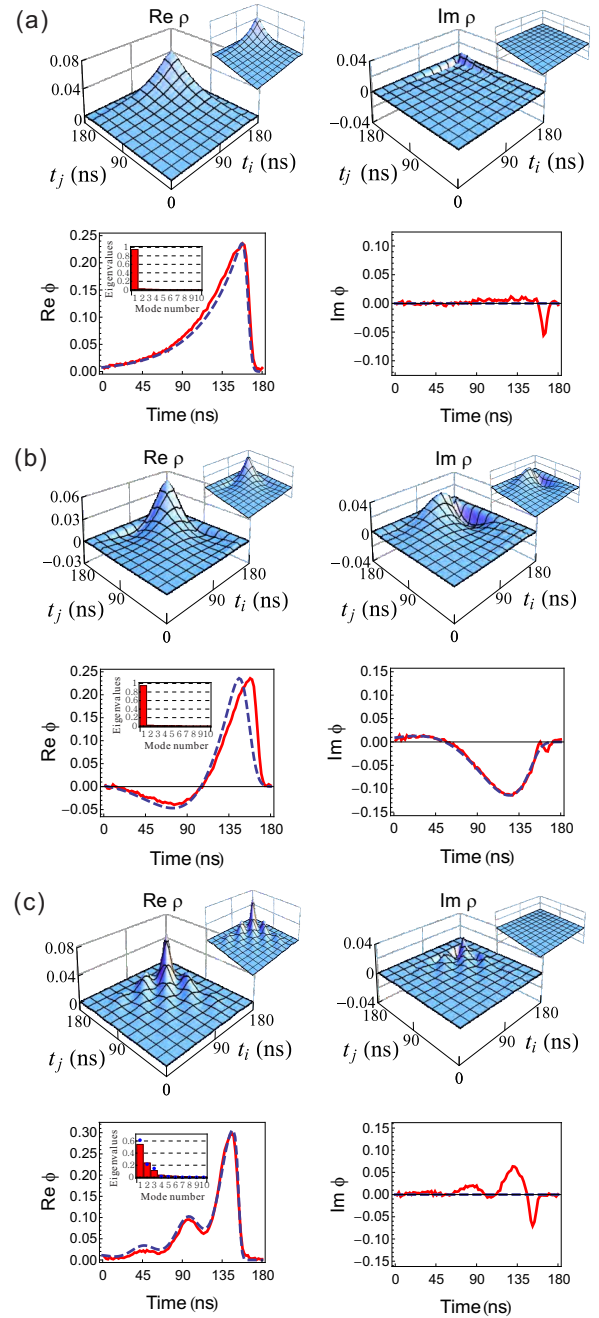


FIG. 3. Experimentally reconstructed temporal modes and their theoretical predictions for the cases without modulation (a), with virtual phase modulation (b), and with phase-randomized EOM modulation (c). For each case, the top two panels show the real (left) and imaginary (right) parts of the TDM, with the insets showing corresponding theoretical plots. Lower two panels show the TDM's primary eigenvector as reconstructed from experimental data (solid red) and theoretical modeling (dashed blue). The insets in the lower left panels show the distribution of eigenvalues (red bars) obtained experimentally. Without EOM modulation (a, b), the theoretically expected mode is pure so the TDM is expected to have only one nonvanishing eigenvector. In the case with EOM modulation (c), the TDM is mixed and the solid blue dots in the inset show theoretical eigenvalues. The trigger photon arrives at $t = 155$ ns.

and CIFAR. AL is a CIFAR Fellow. ZQ is supported by the China Scholarship Council.

and G. Leuchs, New J. Phys. **15**, 123008 (2013).

SUPPLEMENTARY MATERIAL

Derivation of temporal wavefunction

The theoretical TMF for the single photon can be obtained as follows. The biphoton generated by the four-wave mixing process with an infinite gain bandwidth can be represented as

$$|\Psi\rangle = \int |1_{\omega_s}, 1_{\omega_i}\rangle \delta(\omega_s + \omega_i - 2\omega_p) d\omega_s d\omega_i \quad (11)$$

where indices s , i and p correspond to signal, idler and pump respectively. The amplitude transmission function of the cavity in the neighborhood of its resonance can be expressed as a function of the detuning of the beam from the cavity resonance frequency $\delta_i = \omega_c - \omega_i$ as $T(\delta_i) = \sqrt{2/\pi\gamma}(1 - 2i\delta_i/\gamma)^{-1}$, where γ is the linewidth of the cavity. Subjecting the idler channel to transmission through this cavity, state (11) transforms into:

$$|\Psi'\rangle = \sqrt{\frac{2}{\pi\gamma}} \int \frac{1}{1 - 2i\frac{\delta_i}{\gamma}} \delta(\omega_s + \omega_i - 2\omega_p) |1_{\omega_s}, 1_{\omega_i}\rangle d\omega_s d\omega_i. \quad (12)$$

Subsequent idler photon detection at time t_i will project the signal onto the state $|\phi_s\rangle = \langle 1_{t_i} | \Psi' \rangle$ where $|1_{t_i}\rangle = \int |1_{\omega_i}\rangle e^{i\delta_i t_i} d\omega_i$. Assuming that the detection event happens at $t_i = 0$, the resultant state in the signal channel in the frequency domain can be expressed as

$$|1_{\phi_s}\rangle = \langle 1_{t_i=0} | \Psi' \rangle = \sqrt{\frac{2}{\pi\gamma}} \int \frac{1}{1 + 2i\frac{\delta_s}{\gamma}} |1_{\omega_s}\rangle d\omega_s, \quad (13)$$

where $\delta_s = 2\omega_p - \omega_c - \omega_s$ is the detuning of the signal frequency from the central frequency determined by the cavity. Performing a Fourier transform on Eq. (13), we find the temporal mode (7) of the signal photon:

$$|1_{\phi_s}\rangle = \sqrt{\gamma} \int e^{\gamma t_s/2} \Theta(-t_s) |1_{t_s}\rangle dt_s \quad (14)$$

where $\Theta(\cdot)$ is the step function. This rising exponential mode is similar to that of a cavity enhanced photon studied in Ref. [23].

* LVOV@ucalgary.ca

- [1] N. Gisin, G. Ribordy, W. Tittel, and H. Zbinden, Rev. Mod. Phys. **74**, 145 (2002).
- [2] D. Bouwmeester, J.-W. Pan, K. Mattle, M. Eibl, H. Weinfurter, and A. Zeilinger, Nature **390**, 575 (1997).
- [3] L.-M. Duan, M. Lukin, J. I. Cirac, and P. Zoller, Nature **414**, 413 (2001).
- [4] E. Knill, R. Laflamme, and G. J. Milburn, Nature **409**, 46 (2001).
- [5] F. Grosshans and P. Grangier, Eur. Phys. J. D **14**, 119 (2001).
- [6] T. Aichele, A. I. Lvovsky, and S. Schiller, Eur. Phys. J. D **18**, 237 (2002).
- [7] M. Keller, B. Lange, K. Hayasaka, W. Lange, and H. Walther, Nature **431**, 1075 (2004).
- [8] K. Mølmer, Phys. Rev. A **73**, 063804 (2006).
- [9] M. Sasaki and S. Suzuki, Phys. Rev. A **73**, 043807 (2006).
- [10] A. I. Lvovsky and M. G. Raymer, Rev. Mod. Phys. **81**, 299 (2009).
- [11] J. S. Lundeen, B. Sutherland, A. Patel, C. Stewart, and C. Bamber, Nature **474**, 188 (2011).
- [12] C. Polycarpou, K. Cassemiro, G. Venturi, A. Zavatta, and M. Bellini, Phys. Rev. Lett. **109**, 053602 (2012).
- [13] A. MacRae, *An Atomic Source of Quantum Light*, Ph.D. thesis, University of Calgary (2012).
- [14] A. MacRae, T. Brannan, R. Achal, and A. I. Lvovsky, Physics in Canada **68**, 137 (2012).
- [15] O. Morin, C. Fabre, and J. Laurat, Phys. Rev. Lett. **111**, 213602 (2013).
- [16] Although single photons associated with a certain moment in time are ill-defined, treatment (1) is approximately valid as long as the spectral width of the photon is much less than its frequency. See M.V. Fedorov *et al.*, Phys. Rev. A **72**, 032110 (2005) for a detailed discussion of this matter.
- [17] A. MacRae, T. Brannan, R. Achal, and A. Lvovsky, Phys. Rev. Lett. **109**, 033601 (2012).
- [18] P. Palittapongarnpim, A. MacRae, and A. Lvovsky, Rev. Sci. Instrum. **83**, 066101 (2012).
- [19] R. Kumar, E. Barrios, A. MacRae, E. Cairns, E. Huntington, and A. Lvovsky, Opt. Comm. **285**, 5259 (2012).
- [20] J. Appel, A. MacRae, and A. Lvovsky, Meas. Sci. Technol. **20**, 055302 (2009).
- [21] See supplementary information.
- [22] P. Kolchin, C. Belthangady, S. Du, G. Y. Yin, and S. E. Harris, Phys. Rev. Lett. **101**, 103601 (2008).
- [23] M. Bader, S. Heugel, A. L. Chekhov, M. Sondermann,